Chinese Journal of Aeronautics, (2023), 36(6): 256–265

Chinese Society of Aeronautics and Astronautics
& Beihang University

Chinese Journal of Aeronautics

cja@buaa.edu.cn
www.sciencedirect.com

Optimal planning for a multi-debris active removal mission with a partial debris capture strategy

Jia GUO, Zhaojun PANG *, Zhonghua DU

School of Mechanical Engineering, Nanjing University of Science and Technology, Nanjing 210094, China

Received 17 May 2022; revised 13 July 2022; accepted 22 September 2022
Available online 10 March 2023

KEYWORDS

Debris capture strategy;
Genetic algorithm;
Multi-debris active removal;
Space debris

Abstract In this paper, a new mission model, called a multi-debris active removal mission with partial debris capture strategy, is proposed. The model assumes that a platform only captures part of the scheduled debris at a time and then releases these debris pieces to a disposal orbit. This process is then repeated until all of the scheduled debris is removed. A genetic algorithm with a multi-parameter concatenated coding method is designed to optimize the plan of a multi-debris active removal mission with a partial debris capture strategy. A set of six pieces of debris and a set of 10 pieces of debris are selected to demonstrate the proposed planning method. The result confirms the effectiveness of the genetic algorithm with the multi-parameter concatenated coding method. The new mission model provides a more comprehensive decision-making framework than the existing mission models and makes it possible to further decrease mission costs.

1. Introduction

Space debris problems are the result of human space activities. A large amount of space debris has become a threat to space assets.[1–4] For example, space debris slammed into the International Space Station and left a hole in its robotic arm in 2021.[5] To protect the space environment, the Inter-Agency space Debris coordination Committee (IADC) published "IADC Space Debris Mitigation Guidelines (Third revision)" in 2021.[6] This policy document would limit debris released during normal operations from then on, but it is unable to decrease the amount of the existing space debris. If no measures are adopted to de-orbit the existing debris, the space environment will be much worse because of Kessler syndrome.[7]

Research suggests that removing a few large debris pieces per year can effectively mitigate the debris growth problem.[8] Therefore, many Active Debris Removal (ADR) methods are being studied.[9] In recent years, research focusing on single debris removal has obtained some success,[10–13] and some methods have been tested on orbit.[14,15] Multi-debris ADR missions have been introduced to reduce launch costs and shorten spacecraft preparation process. A multi-debris ADR mission plan requires the determination of how to remove multiple pieces of debris within a mission.[16,17]

A mission model is important for multi-debris ADR mission planning since both the optimization variables and the

* Corresponding author.
E-mail address: pangzj@njust.edu.cn (Z. PANG).

Peer review under responsibility of Editorial Committee of CJA.

https://doi.org/10.1016/j.cja.2023.03.013

cost function are determined by the mission model itself. There are currently two models for a multi-debris ADR mission.[18–22] In the first mission model, the platform only captures one piece of debris at a time and then releases the debris to a "disposal orbit" with a low perigee. This process is repeated until all of the scheduled debris pieces are removed. In the second mission model, the platform needs to capture all of the scheduled debris and bring the debris together to disposal orbit. The multi-debris ADR mission planning problem with one of the above-mentioned models can be seen as a Time-Dependent Traveling Salesman Problem (TD-TSP). The optimization variables are the debris removal sequence and the transfer trajectory. Many studies have been conducted for multi-debris ADR missions. The target access sequence was optimized in the study of Alfriend et al.,[23] but this optimization did not involve transfer trajectory optimization. Jorgensen and Sharf[21] proposed a high-accuracy, low-thrust transfer trajectory design method for multi-debris ADR missions, but the debris removal sequence was not optimized. In Refs.[16–18,24–26], the optimization of both the debris removal sequence and the transfer trajectory was performed. Additionally, the optimization of the transfer trajectory is usually replaced by the optimization of the transfer time, since the latter can determine the transfer trajectory. To improve computational efficiency, Artificial Neural Networks (ANNs) have been adopted to quickly estimate the transfer cost.[20] It can be seen that most studies are focused on how to find the optimal plan for a multi-debris ADR mission. However, studies for mission model improvement are rare.

In this paper, a new mission model called "multi-debris ADR mission with Partial Debris Capture Strategy (PDCS)" is proposed. Two areas have been improved in this mission model. One is that the platform can choose between releasing debris and capturing the next piece of debris. The other is that the waiting time is added to optimization variables to select a suitable departure position. This improved mission model provides a flexible decision making framework for decreasing mission costs and is closer to reality. The multi-debris ADR mission with the PDCS planning problem is a variant of TD-TSP. Optimization methods proposed in previous works are not suitable for this problem. Therefore, a genetic algorithm with a multi-parameter concatenated coding method is designed in this research to deal with the problem.

The remaining content is organized as follows. The existing models and the new model for the multi-debris ADR mission are detailed in Section 2. The genetic algorithm with a multi-parameter concatenated coding method is explained in Section 3. The simulation results and the analysis of these results are given in Section 4. Section 5 summarizes the methodology and draws conclusions.

2. Mission model

2.1. Existing mission model

The mission model is used to guide optimization efforts for multi-debris ADR missions. Previous studies often used the following two mission models to design mission plans: the multi-debris ADR mission with the Single Debris Capture Strategy (SDCS)[21] and the multi-debris ADR mission with the All Debris Capture Strategy (ADCS).[22] For each mission model, debris must be released to a disposal orbit. Usually, the altitude of a disposal orbit is set to 200 km which ensures that debris in Low Earth Orbit (LEO) enters the Earth's atmosphere and burns up within one year.

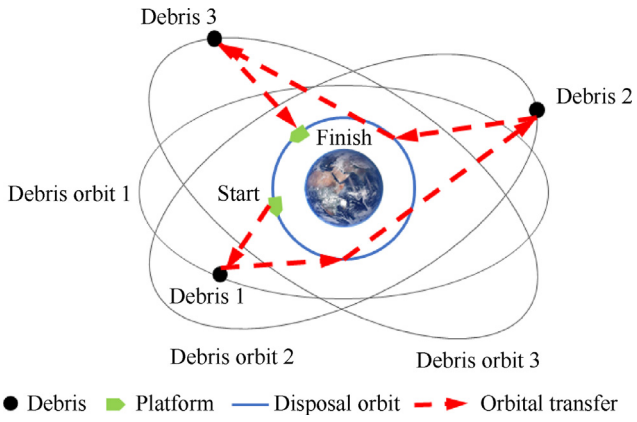

Fig. 1 Scheme of single debris capture strategy.

A multi-debris ADR mission with the SDCS is depicted in Fig. 1. The platform captures only one piece of debris at a time. Once a piece of debris has been captured, the platform carries the debris to a disposal orbit immediately. After the debris is released, the platform transfers to the orbit of the next piece of debris and goes on to the next debris removal phase.

Fig. 2 presents the process of a multi-debris ADR mission with the ADCS. After capturing a piece of debris, the platform transfers to the orbit of the next piece of debris and captures it directly instead of releasing the captured debris to a disposal orbit. At the end of the mission, all of the scheduled debris will be captured and the platform will carry the debris to a disposal orbit together.

The SDCS and the ADCS have their own merits and flaws. In the SDCS, the total mass of the platform can be maintained at a lower level, but the platform performs a transfer somewhat frequently because each piece of debris has to be brought to a disposal orbit separately. The transfer times are cut down in the ADCS, but the total mass will reach a high level in the latter part of a complete multi-debris ADR mission because of the accumulation of debris.

Because neither a high mass load nor frequent orbital transfers are beneficial to a multi-debris ADR mission, a compromise between the SDCS and the ADCS may present a better performance. For the above reasons, a new mission model is proposed in Section 2.2.

As a supplement, there is another debris processing strategy known as a Deorbiting Kit Strategy (DKS). In this strategy, the platform attaches a "deorbit-kit" to the debris after a rendezvous. This kit is responsible for the deorbiting of the debris.[18] However, stabilizing the debris and attaching a deorbit-kit are cumbersome and there is no mature technology to achieve this.[21] Therefore, the strategy is not discussed in this paper.

2.2. Partial debris capture strategy

The Partial Debris Capture Strategy (PDCS) is proposed in this paper to balance transfer times and transfer loads. Its flow

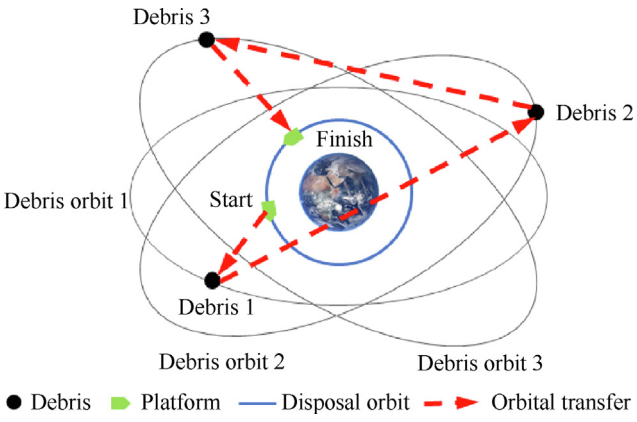

Fig. 2 Scheme of all debris capture strategy.

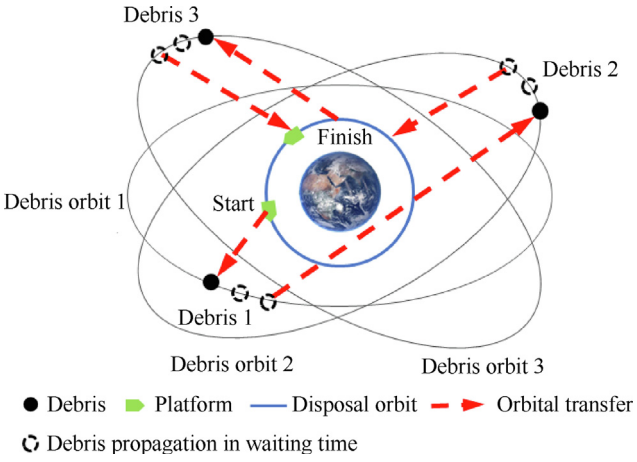

Fig. 3 Scheme of partial debris capture strategy.

is shown in Fig. 3. The platform captures part of but not all of the debris at a time and releases the debris to disposal orbit afterward. This process is repeated several times until all of the scheduled debris pieces are removed. The new strategy has fewer transfers compared with the SDCS and avoids the overweight condition caused by debris accumulation compared with the ADCS. Furthermore, the waiting time is considered in the PDCS since it has a significant influence on transfer trajectory.[27,28] In the SDCS and the ADCS, the variables usually are deorbit sequence and transfer time and don't include the waiting time.[18,21] In the PDCS, the platform needs to wait in its current orbit until a suitable time is reached to start transfer. Hence, the multi-debris ADR mission with PDCS is more practical and is favorable for decreasing mission costs.

Assuming that n pieces of debris are considered for removal in the multi-debris ADR mission with the PDCS, the symbols of the mission parameters are set as shown below. The debris removal sequence can be represented by a $n \times 1$ vector $\boldsymbol{d} = [d(1), d(2), \cdots, d(n)]^T$ such that its ith element $d(i), 1 \leqslant d(i) \leqslant n$ specifies the index of the debris to be removed in the ith segment of the mission. Let t_i represent the moment when the platform rendezvouses with Debris i, and it is assumed that the time when Debris i is captured is the same as t_i. At the beginning of the mission, the platform is delivered to the first debris item by the launch vehicle without an energy cost to itself and this moment is denoted as $t_1 = 0$. For each Debris i, $\Delta t_{\mathrm{w}}(i)$ denotes the waiting time before the beginning of the transfer. $\Delta t_{\mathrm{m}}(i)$ denotes the transfer time. $b(i)$ is set to decide whether the platform releases the captured debris to a disposal orbit after Debris i is captured. If $b(i) = 1$, the platform transfers to a disposal orbit and the debris removal process is shown in Fig. 4(a). Otherwise, if $b(i) = 0$, the debris removal process is shown in Fig. 4(b). A Hohmann transfer is adopted when the platform moves to a disposal orbit and the Hohmann transfer durations are recorded as $\Delta t_{\mathrm{h}}(i)$. In Fig. 4(b), $\Delta t_h(i)$ is equal to 0 since a Hohmann transfer is not carried out. Then, the moment when debris $i+1$ is captured can be expressed as

$$t_{i+1} = t_i + \Delta t_h(i) + \Delta t_w(i) + \Delta t_m(i) \tag{1}$$

The total duration Δt^* is constrained by a maximum mission duration $T_{\max}$:

$$\begin{cases} \Delta t^* = \sum_{i=1}^{n-1} \Delta t_{\mathrm{h}}(i) + \sum_{i=1}^{n-1} \Delta t_{\mathrm{w}}(i) + \sum_{i=1}^{n-1} \Delta t_{\mathrm{m}}(i) \\ \Delta t^* \leqslant T_{max} \end{cases} \tag{2}$$

Unlike other astrodynamics problems, the total velocity increment Δv cannot be a substitute for the propellant consumption as a cost function since some dry mass variation occurs during the mission because of the debris capture/release.[18] Therefore, the momentum increment Δp is employed in this study to reflect the influence of the mass variation and keep the transfer model simple to minimize the computational time. However, the momentum increment is representative of propellant consumption, and therefore, it can be easily varied for future use-cases. Similarly, there is also a constraint for momentum:

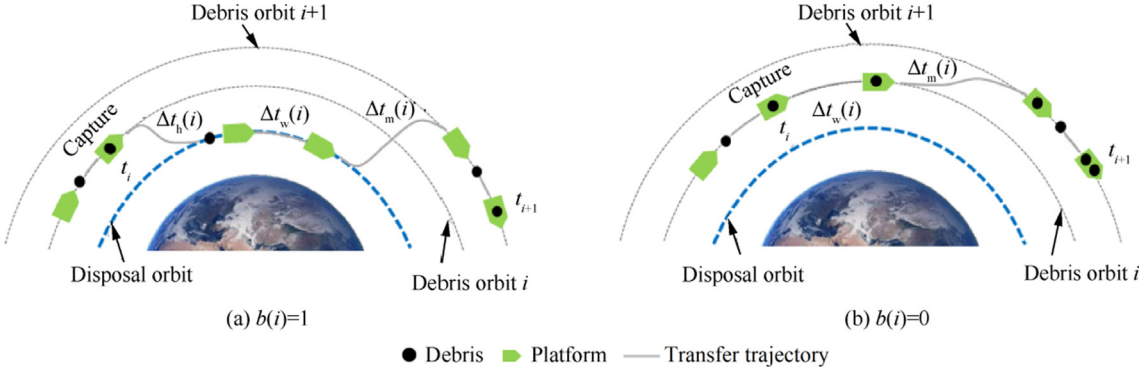

Fig. 4 Two possible transfer processes after capturing one piece of debris.

$$\begin{cases} \Delta p^* = \sum_{i=1}^{n} \Delta p_{\mathrm{h}}(i) + \sum_{i=1}^{n-1} \Delta p_{\mathrm{m}}(i) \\ \Delta p^* \leqslant \Delta p_{max} \end{cases} \tag{3}$$

where $\Delta p_{\mathrm{h}}(i)$ is the momentum increment caused by the Hohmann transfer when the platform moves from the orbit of Debris i to a disposal orbit. If the Hohmann transfer is not carried out, $\Delta p_{\mathrm{h}}(i)$ is equal to 0. $\Delta p_{\mathrm{m}}(i)$ is the momentum increment arising during $\Delta t_{\mathrm{m}}(i)$. $\Delta p_{\max}$ is maximum mission momentum increment.

The cost function used for the selection of the optimal mission plan can be defined as

$$J = \alpha \frac{\Delta p^*}{\Delta p_{\max}} + (1-\alpha)\frac{\Delta t^*}{T_{\max}} \qquad \alpha \in [0,1] \tag{4}$$

The weighting factor α can be chosen by the mission designer.

The multi-debris ADR mission with partial debris capture strategy can be seen as a mixed-integer optimization problem, and the optimal planning model is proposed as follows:

$$\min J = \alpha \frac{\Delta p^*}{\Delta p_{\max}} + (1-\alpha)\frac{\Delta t^*}{T_{\max}}$$
$$s.t. \begin{cases} b(i) \in \{0,1\} & i = 1,2,...,n \\ d(i) \in \{0,1,...,n\} & i = 1,2,...,n \\ d(i) \neq d(j) & i,j = 1,2,...,n \quad \text{and} \quad i \neq j \\ \Delta t_w(i) \in [\Delta t_w^{\min}, \Delta t_w^{\max}] & i = 1,2,...,n \\ \Delta t_m(i) \in [\Delta t_m^{\min}, \Delta t_m^{\max}] & i = 1,2,...,n \\ \Delta t^* \leqslant T_{\max} \\ \Delta p^* \leqslant \Delta p_{\max} \end{cases} \tag{5}$$

where $[\Delta t_w^{\min}, \Delta t_w^{\max}]$ is the value range of $\Delta t_w(i)$, and $[\Delta t_m^{\min}, \Delta t_m^{\max}]$ is the value range of $\Delta t_m(i)$. These two value ranges are used to ensure that the constraint of $\Delta t^* \leqslant T_{\max}$ can be satisfied.

2.3. Drift orbit transfer

Many approaches have been adopted in multi-debris ADR mission plans to estimate the cost of transferring between a pair of debris pieces, such as a Lambert transfer or a low-thrust transfer.[24,29] Cerf[26] presented a drift-orbit transfer approach that used the natural procession of the J_2 zonal term on the intermediate orbit, called the drift orbit, to stay in place until the targeted Right Ascension of Ascending Node (RAAN, represented by Ω) was reached. This approach has two significant advantages. One is reduction of energy consumption because the platform does not require energy to change RAAN, and the other is lower computational complexity for avoiding numerical integration and equation solving. Because of these advantages, the drift-orbit transfer approach has been used in many studies, and this study also uses this approach. Additionally, the phasing along the orbit between the platform and the debris is neglected in the transfer model for the phase maneuver because it only lasts for a few revolutions.[20]

Assuming that the platform is going to transfer to the orbit of Debris $i + 1$, the drift-orbit transfer consists of three steps:

Step 1. The platform transferring from its orbit to the drift orbit, as shown in Fig. 5(a).

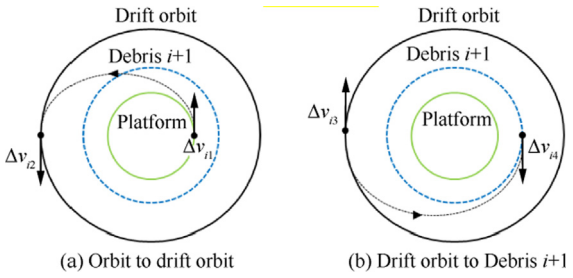

Fig. 5 Transfer maneuvers and successive orbits.

Step 2. Staying in the drift orbit until the coincidence of Ω with the orbit of Debris $i + 1$.

Step 3. Transferring from the drift orbit to the orbit of Debris $i + 1$, as shown in Fig. 5(b).

A Hohmann transfer is performed in Steps 1 and 3 with impulsive velocity increments applied at the apsides. If an inclination change is required in addition to the change of altitude, the inclination maneuver is completed along with the altitude maneuver as Ref.[18] did, as Fig. 6 shown, where, $\boldsymbol{v}_{\mathrm{initial}}$ is the velocity vector before the maneuver, $\boldsymbol{v}_{\mathrm{final}}$ is the velocity vector after the maneuver, $\Delta \boldsymbol{v}$ is the velocity increment of the maneuver, ΔI is the variation of inclination.

Given the semi-major axis a, the eccentricity e, and the orbit inclination I, the secular precession rate of Ω caused by the J_2 zonal term of the equatorial bulge perturbing force of the Earth is expressed as

$$\dot{\Omega} = -C_{J2} \cos I \cdot a^{-\frac{7}{2}} (1-e^2)^{-2} \tag{6}$$

with

$$C_{J2} = \frac{3}{2} J_2 \sqrt{\mu_{\mathrm{E}}} \cdot R_{\mathrm{E}}^2 \tag{7}$$

where $J_2 = 1.0826 \times 10^{-3}$ represents the second zonal harmonics of the Earth's gravitational potential; $R_E = 6378137$ m is the Earth's radius; $\mu_{\mathrm{E}} = 398600.5$ $\mathrm{km^3 \cdot s^{-3}}$ is the gravitational parameter of the Earth.

The draft orbit aims to provide a large enough RAAN secular precession rate for the platform to coincide with the RAAN of the target debris. Given the transfer time $\Delta t_{\mathrm{m}}(i)$, the constraint below should be satisfied:

$$\Omega_{\mathrm{p}}(t_i + \Delta t_{hi} + \Delta t_{wi}) + \Delta t_{\mathrm{m}i} \dot{\Omega}_{\mathrm{d}} = \Omega_{i+1}(t_i + \Delta t_{\mathrm{h}i} + \Delta t_{\mathrm{w}i}) + \Delta t_{\mathrm{m}i} \dot{\Omega}_{i+1} \tag{8}$$

where $\Omega_{\mathrm{p}}(t_i + \Delta t_{\mathrm{h}i} + \Delta t_{\mathrm{w}i})$ and $\Omega_{i+1}(t_i + \Delta t_{\mathrm{h}i} + \Delta t_{\mathrm{w}i})$ are the RAAN of the platform and Debris $i + 1$, respectively, when the platform is preparing to transfer to the orbit of Debris $i + 1$; $\Delta t_{\mathrm{h}i}$, $\Delta t_{\mathrm{w}i}$ and $\Delta t_{\mathrm{m}i}$ are equal to $\Delta t_{\mathrm{h}}(i)$, $\Delta t_{\mathrm{w}}(i)$ and

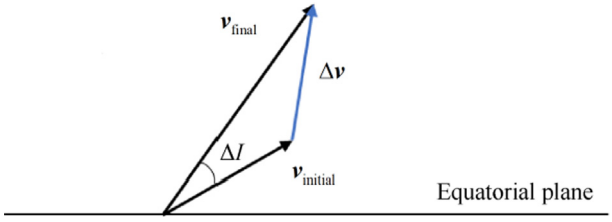

Fig. 6 Simultaneous inclination and shape change.

$\Delta t_m(i)$, respectively; $\dot{\Omega}_d$ is the RAAN secular precession rate of the drift orbit; $\dot{\Omega}_{i+1}$ refers to the RAAN secular precession rate of the orbit where Debris $i + 1$ is located.

3. Genetic algorithm with multi-parameter concatenated coding method

Because two new kinds of variables $b(i)$ and $\Delta t_w(i)$ are added to the mission model, the existing optimization methods are not suitable for the new mission model. In previous works, a branch and bound algorithm has been used to optimize the mission plan because it can find the optimum solution effectively when only $d(i)$ and $\Delta t_m(i)$ need to be optimized. However, there are four kinds of variables in the new mission model and a combinatorial explosion will lead to a huge computational burden. Therefore, a Genetic Algorithm (GA) is adopted in this study since it can perform simultaneous optimization for multiple variables and execute a global search[30,31].

The coding method is crucial for genetic algorithm because it determines the form of the genes and has an impact on the other operators. It largely determines the computational efficiency of the genetic algorithm. In general, the binary coding method is enough to encode the mission variables. However, it cannot satisfy the encoding requirements of the variables in the multi-debris ADR mission with the PDCS. The binary coding method may generate many genes without an efficient solution. For example, the rendezvous time t_i is encoded by the binary coding method in the study of Liu and Yang[32]. It often happens that $t_{i+1} < t_i$, which corresponds to the gene but is impossible in reality. However, multi-debris ADR planning is a mixed-integer optimization problem since $b(i)$, $d(i)$ are integer variables and $\Delta t_m(i)$, $\Delta t_w(i)$ are continuous variables. If the binary coding method is applied to a continuous variable, the gene cannot meet the precision requirement when the length of the gene is short. The precision can be improved by using a longer gene, but it will lead to a dramatic increase in the search space. A variable that ranges between -250 and 250 is taken as an example. When this variable is required to be accurate to five decimal places, the gene will be a 26-digit number, as shown in

$$2^{25} = 33554432 < \frac{500}{0.00001} = 50000000 < 67108864 = 2^{26} \quad (9)$$

If there are 100 variables, the search space will go up to approximately 2^{2600}. Such a huge search space will reduce the efficiency of computation.

Due to the above reasons, the Multi-Parameter Concatenated Coding Method (MPCCM) is adopted in this study. Variables are encoded with different basic coding methods, and an individual gene is built by concatenating the codes of the variables. However, there is no general guiding theory to help determine a basic coding method reasonably for each variable and it is difficult for a multi-parameter concatenated coding method to be applied[33]. To solve this problem, coding methods for $b(i)$, $d(i)$, $\Delta t_w(i)$, and $\Delta t_m(i)$ are determined by comprehensively considering the multi-debris ADR mission characteristics and the operation process of the genetic algorithm.

With only two possible values, 1 and 0, $b(i)$ is coded with the binary coding method because this coding method is easy to operate. Furthermore, there will not be invalid solutions when crossover and mutation operations are performed. It is worth noting that $b(n)$ is fixed as 1 because debris must be released when the mission is finished.

$d(i)$ is coded with the symbolic coding method. The code is generated by connecting indexes of debris in the order in which they are captured. In this way, the code of $d(i)$ has a shorter length and it is easy to be decoded.

$\Delta t_w(i)$ and $\Delta t_m(i)$ are coded with the float-point coding method because they are continuous variables. When the float-point coding method is adopted, each value of a gene is represented by a floating-point number within a certain range. Hence, the precision is guaranteed with a shorter gene length and the constraint is convenient to be set up.

Taking one gene in the six-debris ADR mission as an example, the code is given in Fig. 7.

As shown in Fig. 7, the gene is divided into four parts corresponding to four kinds of variables. The first number of the first part is 0 which means that the platform will prepare for capturing the second debris directly but not releasing the debris to a disposal orbit. The first number of the second part is 6. This means that the index of the first debris to be captured is 6. The first number of the third part is 8, so $\Delta t_w(1)$ is equal to 8 days. Similarly, $\Delta t_m(1)$ is equal to 52 days because the first number of the fourth part is 52. In this way, the meanings of all figures in the gene can be explained.

In summary, the genetic algorithm with the multi-parameter concatenated coding method designed in this study has the following advantages:

(1) The simultaneous optimization of the four kinds of variables is achieved and the computational burden is decreased compared with a branch and bound algorithm.
(2) The computational efficiency is improved compared with a genetic algorithm with the binary encoding method only.

4. Results and discussion

4.1. Scenario setting

Two mission scenarios are set in this study to validate a multi-debris ADR mission model with different capture strategies and the genetic algorithm with the MPCCM. The first mission scenario is that a platform needs to remove six pieces of debris in one year. The second mission scenario is that a platform needs to remove 10 pieces of debris in two years. Two different

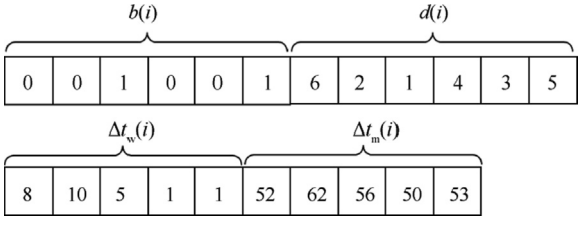

Fig. 7 One gene in six-debris ADR mission.

Table 1 Debris list for the first scenario.

Index	a(km)	I(°)	$e(10^{-3})$	Ω(°)
1	7158.0	86.3	0.8	304.1
2	7011.6	86.4	2.4	301.0
3	7142.8	86.3	1.3	302.8
4	7154.2	86.3	1.4	298.2
5	7157.4	86.4	1.5	312.2
6	7133.1	86.3	0.6	295.0

Table 2 Debris list for the second scenario.

Index	a(km)	I(°)	$e(10^{-3})$	Ω(°)
1	7030.5	98.0	0.1	221.1
2	7055.3	98.1	0.1	188.3
3	7080.0	98.2	0.1	164.4
4	7104.4	98.3	0.3	235.0
5	7128.5	98.4	0	174.7
6	7152.5	98.5	0.1	194.1
7	7176.3	98.6	0.1	149.0
8	7200.3	98.7	0.1	180.3
9	7223.2	98.8	0.2	200.6
10	7246.4	98.9	0.1	191.0

Table 3 Parameters of constraint.

Parameter name	The first scenario	The second scenario
Maximum mission momentum increment $\Delta p_{\max}$ (10^7kg · m/s)	4	8
Maximum mission duration $T_{\max}$ (d)	365	730
Value range of $\Delta t_{\mathrm{w}}(i)$ (d)	$[0, 10]$	$[0, 10]$
Value range of $\Delta t_{\mathrm{m}}(i)$ (d)	$[50, 61]$	$[50, 71]$

debris lists are extracted from Refs.[25,26] for the two mission scenarios as detailed in Tables 1 and Table 2, where, a is the semi-major axis, I is the orbital inclination, e is the orbital eccentricity.

The constraint parameters are listed in Table 3. The maximum mission momentum increment is determined according to the maximum value of the individuals in the initial population. The value range of $\Delta t_{\mathrm{w}}(i)$ and the value range of $\Delta t_{\mathrm{m}}(i)$ are set to ensure that Δt^* will not surpass $T_{\max}$. According to Ref.[26] and computation, $\Delta t_{\mathrm{m}}(i)$ needs to be larger than 50 days or else $\Delta p_{\mathrm{m}}(i)$ will grow steeply. The weighting factor is $\alpha = 0.5$. The mass of the platform is $M_{\mathrm{platform}} = 3000$ kg. The parameters of the GA are defined in Table 4.

All of the described tasks are performed on a Windows system PC with one CPU (Intel(R) Core (TM) i5-9300H @2.4 GHz), and the amount of RAM is 16 GB.

4.2. Results of the first scenario

A numerical experiment with the condition that the mass of a single piece of debris is 1000 kg is conducted to test the genetic algorithm which is discussed in Section 3. Fig. 8 plots the performance of the genetic algorithm with the MPCCM. The minimum objective function value of the initial population is 0.5698. After optimization, the minimum objective function value goes down to 0.4877 at the 168th generation, which is a decrease of 14.4%. The computation time is 1.2 s. Additionally, a traditional genetic algorithm that adopts only the binary coding method is employed for comparison. The result is also shown in Fig. 8. The minimum objective function value generated by the traditional genetic algorithm is 0.4927. It consumes 6.9 s of computation time. The genetic algorithm with the MPCCM has a lower cost and its computational efficiency is 5.75 times higher than that of the traditional genetic algorithm.

Table 4 Parameters of GA.

Parameter name	Parameter value
Population size	100
Termination conditions	Generations $\geqslant$ 200
Crossover rate	0.7
Mutation rate	0.1

The gene of the optimal individual is shown in Fig. 9. According to this gene, Fig. 10 plots the mission process. It can be seen that after capturing the first piece of debris, the platform releases this debris to a disposal orbit as $b(1) = 1$. Then, the platform moves to capture five pieces of debris continuously as $b(2), b(3), b(4), b(5) = 0$, and the five pieces of debris are released to a disposal orbit when the sixth piece of debris is captured as $b(6) = 1$. Correspondingly, the debris removal sequence is 5-1-3-4-6-2.

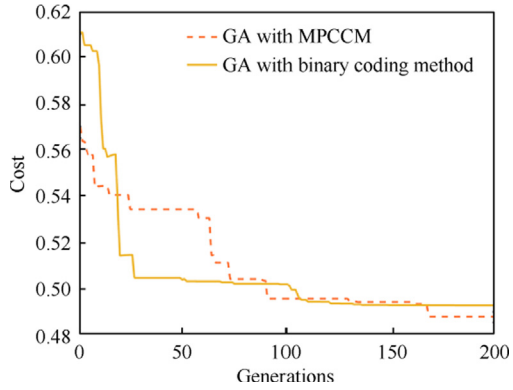

Fig. 8 Optimization result for six-debris ADR mission.

To compare different debris capture strategies and analyze their characteristics, a series of numerical experiments with different single debris masses are conducted. The numerical experiments employ the PDCS, ADCS, ADCS considering waiting time, SDCS, and SDCS considering waiting time for the multi-debris ADR mission. The optimal solutions of these debris capture strategies for different debris mass conditions are generated and their costs are presented in Fig. 11.

It can be seen that the PDCS has the best performance in all debris mass conditions. Compared with the ADCS, the cost of the PDCS is reduced by 5% at least, 23% at most, and 13% on average. Compared with the SDCS, the cost of the PDCS is reduced by 3% at least, 27% at most, and 12% on average. PDCS is obviously superior to the SDCS when the mass of single debris is less than 4000 kg. The superiority of the PDCS compared with ADCS increases along with the increase of the single debris mass. The cost of the ADCS considering the waiting time is lower than the cost of the ADCS but has the same trend as the cost of the ADCS. This phenomenon also appears between the SDCS considering the waiting time and the SDCS.

Fig. 12 shows the relationship between the debris release times and the mass of single debris mass. The debris release times of the ADR mission with the SDCS are always 6. The debris release times of the ADR mission with the SDCS are always one. When the PDCS is adopted, the debris release times tend to rise with the increase of single debris mass.

4.3. Results of the second scenario

The results of optimization for the 10-debris ADR mission are given in Fig. 13. The mass of a single piece of debris is 1000 kg. When the genetic algorithm with the MPCCM is adopted, the cost goes down from 0.6973 to 0.5841, which is a decrease of 16.2%. The computation time is 1.5 s. The cost of the best individual produced by a genetic algorithm with the binary coding method is 0.4927. The computation takes 10.8 s. The genetic algorithm with the MPCCM gives a better result and its computational efficiency is 7.2 times higher than that of the genetic algorithm with the binary coding method.

The gene of the optimal individual for the 10-debris ADR mission is shown in Fig. 14. The corresponding debris removal process is shown in Fig. 15. The platform first brings Debris 3 and Debris 7 to the disposal orbit and then Debris 8, Debris 2, and Debris 5 are removed. Finally, the platform captures Debris 4, Debris 1, Debris 10, Debris 6 and Debris 9 sequentially and releases the five pieces of debris to disposal orbit together.

Fig. 16 plots the cost of the optimal individual for different single debris mass conditions when the PDCS, ADCS, ADCS considering waiting time, SDCS, and SDCS considering waiting time are employed. The PDCS has a lower cost than the other debris capture strategies in all of the debris mass conditions. Compared with the ADCS, the cost of the PDCS is reduced by 4% at least, 28% at most, and 18% on average. Compared with the SDCS, the cost of the PDCS is reduced by 10% at least, 32% at most, and 19% on average. The SDCS has a better performance than the ADCS when the single piece of debris is light. However, the ADCS is superior to the SDCS if the debris is heavy. The ADCS considering waiting time and the SDCS considering waiting time outperform the ADCS and the SDCS respectively. Taking the waiting time into consideration, the cost can be decreased to a certain degree. However, the waiting time cannot affect the tendency since the curves of ADCS/SDCS considering waiting time are almost parallel to the curves of ADCS/SDCS.

The relationship between the debris release times and the single debris mass in the 10-debris ADR mission is shown in Fig. 17. The debris release times of the ADR mission with the SDCS are always 10. The debris release times of the ADR mission with the SDCS are always one. When the PDCS is adopted, the heavier the single debris piece is, the more the debris release actions are.

4.4. Results summary and discussion

Combining the result of the six-debris ADR mission and the 10-debris ADR mission, we can see that the genetic algorithm with the MPCCM only consumes 13%–17% of the computation time of the traditional genetic algorithm. The genetic algorithm with the MPCCM shows its remarkable advantage in computational efficiency. This also shows that the basic coding methods for the variables determined in this research are reasonable. The benefit of the computational efficiency improvement is considerable when other optimization content is

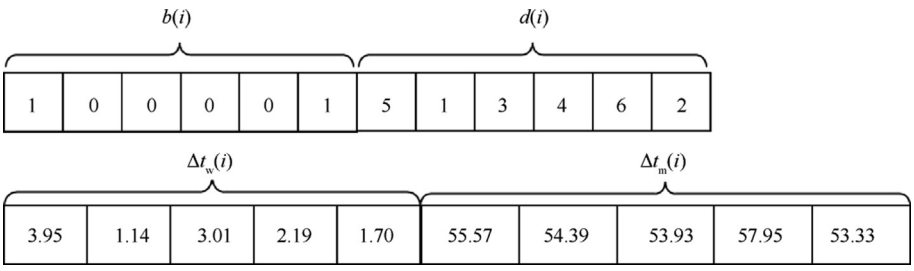

Fig. 9 Gene of optimal individual for six-debris ADR mission.

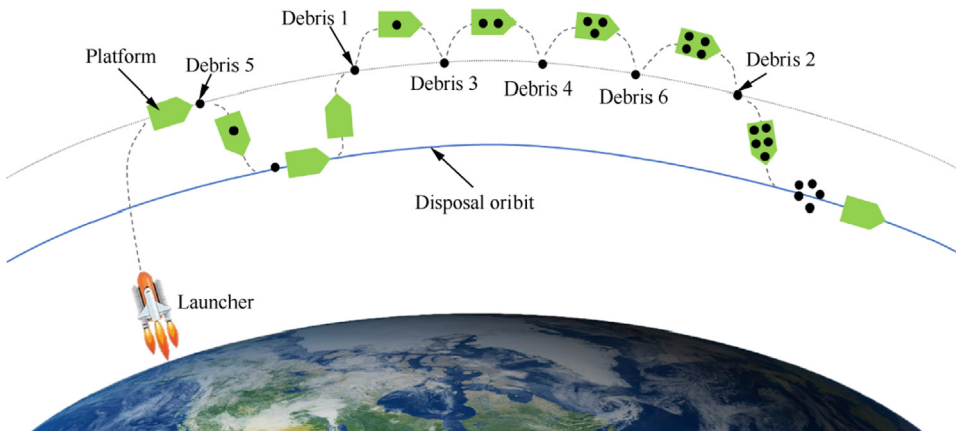

Fig. 10 Debris removal process for six-debris ADR mission.

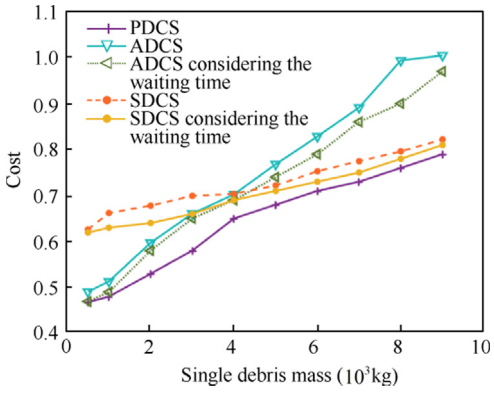

Fig. 11 Optimal result under different debris mass conditions.

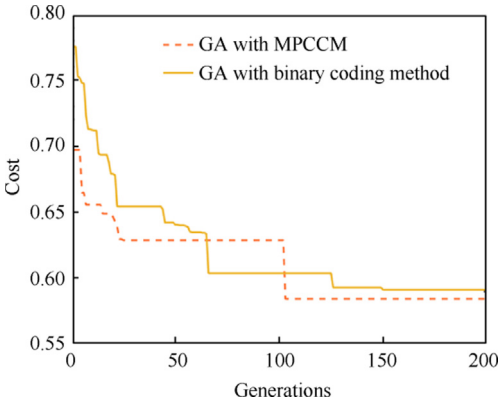

Fig. 13 Optimization result for 10-debris ADR mission.

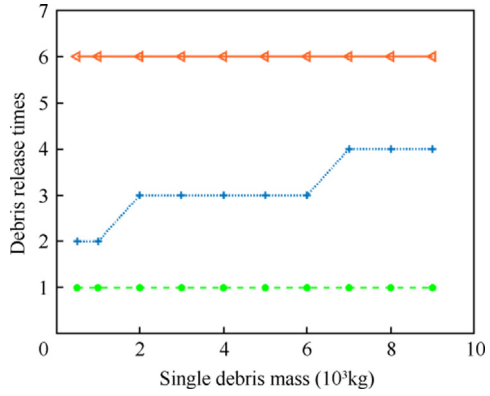

Fig. 12 Debris release times in 6-debris ADR mission.

taken into account, such as in selecting debris from a large number of candidate objects, for which the computation time goes up to several hours. For example, the computation time was 15.2 hours in Ref.[32] which also used a genetic algorithm.

Compared with the ADCS and the SDCS, the PDCS exhibits its obvious advantage in both the six-debris ADR mission and the 10-debris ADR mission since the ADCS and the SDCS can be seen as the special cases of the PDCS, and the PDCS has more flexible choices. The general trend of these debris capture strategies is that their costs rise with the increase of a single debris mass but each has its characteristics. The costs of the ADCS rise rapidly with the increase of a single debris mass because the accumulated debris brings a huge mass load to maneuvers. The SDCS has a higher cost when a single piece of debris is light because the mass of the platform accounts for a substantial part of the total mass and the three strategies have almost the same level of total mass but the SDCS has more maneuvers than the other two strategies. The PDCS achieves a balance between the mass load and the number of maneuvers and provides a better result. When the waiting time is considered in the ADCS and the SDCS, the cost is decreased but the general trend is not changed. This suggests that a reasonable waiting time is beneficial to the decrease of the cost but the main influencing factor of the cost is the debris capture strategy.

In both the 6-debris ADR mission and 10-debris ADR mission, the debris release times tend to rise with the increase of single debris mass. The reason is inferred below. It is obvious that both the huge mass load and the frequent orbital transfers are unbeneficial for cost decrease. Releasing debris can help to reduce the mass load of the maneuvers but it entails more orbital transfers. Because one debris releasing action can unload lots of mass burdens when the debris piece is heavy, the benefit of reducing mass load outweighs the injury of increasing orbital transfers. Therefore, there are more debris release actions when the debris piece is heavy.

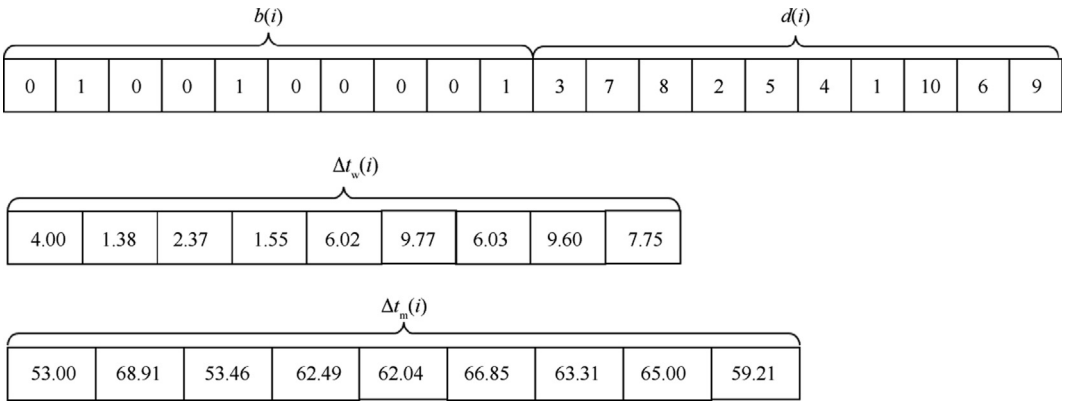

Fig. 14 Gene of optimal individual for 10-debris ADR mission.

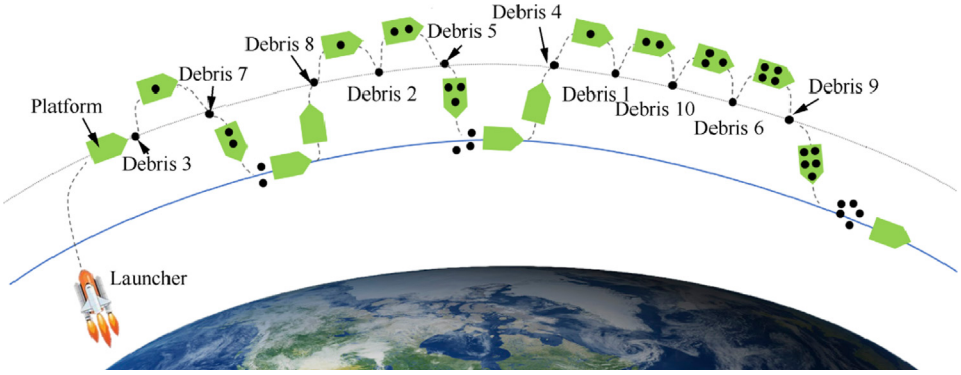

Fig. 15 Debris removal process for 10-debris ADR mission.

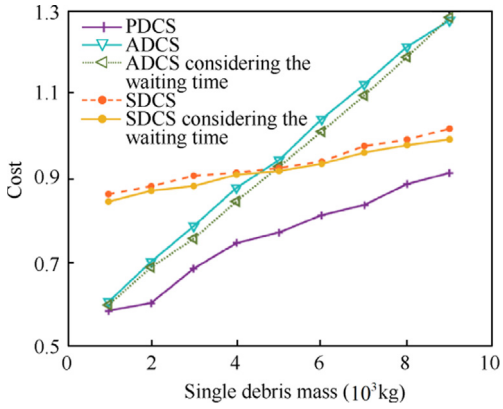

Fig. 16 Optimal result under different debris mass conditions.

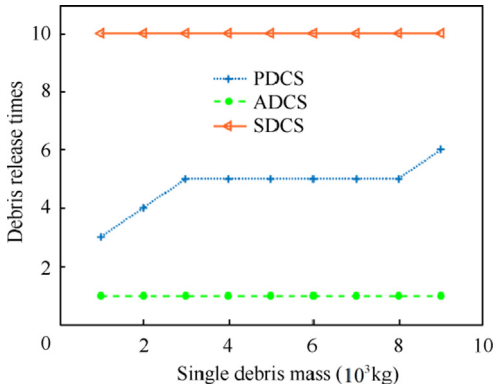

Fig. 17 Debris release times in 10-debris ADR mission.

5. Conclusions

A new mission model called a multi-debris ADR mission with the PDCS is proposed in this paper. The PDCS is developed from the SDCS and the ADCS. PDCS considers the whole mission flow, not just the transfer time scheme and the debris sequence. This makes it possible to perform further optimization based on the optimal solutions of the ADCS and the SDCS. To find the optimal solution to the ADR mission with PDCS, a genetic algorithm with the multi-parameter concatenated coding method is designed in this research. Each variable is assigned one reasonable coding method according to its characteristics.

To verify the effectiveness of the PDCS and the genetic algorithm with the multi-parameter concatenated coding method, a six-debris ADR mission and a 10-debris ADR mission are conducted, while the ADCS and the SDCS are also applied for comparison. The results show that the solution produced based on the PDCS has a lower cost. Compared with the ADCS, the cost of the PDCS is reduced by 3% at least, 28% at most, and 15% on average. Compared with the SDCS, the cost of the PDCS is reduced by 4% at least, 32% at most,

and 16% on average. The computational efficiency of the genetic algorithm with the multi-parameter concatenated coding method is 5–7 times higher than that of the traditional genetic algorithm with the binary coding method. The law is summarized that the platform tends to capture all of the pieces of debris and release them to a disposal orbit together when the debris mass is small because the times of transfer can be reduced in this way. In contrast, the platform tends to release debris immediately once one piece of heavy debris is captured, because performing a transfer with a huge mass load is uneconomic.

Declaration of Competing Interest

The authors declare that they have no known competing financial interests or personal relationships that could have appeared to influence the work reported in this paper.

Acknowledgements

This study was co-supported by the Open Fund Project of Space Intelligent Control Technology Laboratory (No. HTKJ2021KL502010), the Research Project of Space Debris and Near-earth Asteroid Defense Grants, China (No. KJSP 2020010303) and the National Natural Science Foundation of China (No. 11802130).

References

1. Obukhov VA, Kirillov VA, Petukhov VG, et al. Problematic issues of spacecraft development for contactless removal of space debris by ion beam. *Acta Astronaut* 2021;**181**:569–78.
2. Rao HP, Zhong R, Li PJ. Fuel-optimal deorbit scheme of space debris using tethered space-tug based on pseudospectral method. *Chin J Aeronaut* 2021;**34**(9):210–23.
3. Cui J, Shen T, Wei T, et al. Tangling and instability effect analysis of initial in-plane/out-of-plane angles on electrodynamic tether deployment under gravity gradient. *Chin J Aeronaut* 2021;**34**(1):1–9.
4. Han D, Dong GQ, Huang PF, et al. Capture and detumbling control for active debris removal by a dual-arm space robot. *Chin J Aeronaut* 2022;**35**(9):342–53.
5. CBS News. Space junk slams into International Space Station, leaving hole in robotic arm [Internet]. [updated 2021 June 2; cited 2022 May 17]. Available from: https://www.cbsnews.com/news/space-junk-damage-international-space-station/.
6. Inter-Agency Space Debris Coordination Committee. IADC Space Debris Mitigation Guidelines [Internet]. [updated 2021 June 6; cited 2022 May 17]. Available from: https://iadc-home.org/documents_public/view/id/172#u.
7. Kessler DJ, Cour-Palais BG. Collision frequency of artificial satellites: The creation of a debris belt. *J Geophys Res* 1978;**83**(A6):2637.
8. Liou JC, Johnson NL, Hill NM. Controlling the growth of future LEO debris populations with active debris removal. *Acta Astronaut* 2010;**66**(5–6):648–53.
9. Mark CP, Kamath S. Review of active space debris removal methods. *Space Policy* 2019;**47**:194–206.
10. Bischof B, Kerstein L. ROGER - robotic geostationary orbit restorer. Reston: AIAA; 2002. Report No.: IAC-03-IAA.5.2.08.
11. Zhang ZP, Yu ZW, Zhang QW, et al. Dynamics and control of a tethered space-tug system using Takagi-Sugeno fuzzy methods. *Aerosp Sci Technol* 2019;**87**:289–99.
12. Meng ZJ, Wang BH, Huang PF. A space tethered towing method using tension and platform thrusts. *Adv Space Res* 2017;**59**(2):656–69.
13. Okninski A. Solid rocket propulsion technology for de-orbiting spacecraft. *Chin J Aeronaut* 2022;**35**(3):128–54.
14. Forshaw JL, Aglietti GS, Fellowes S, et al. The active space debris removal mission RemoveDebris. Part 1: From concept to launch. *Acta Astronaut* 2020;**168**:293–309.
15. Aglietti GS, Taylor B, Fellowes S, et al. The active space debris removal mission RemoveDebris. Part 2: In orbit operations. *Acta Astronaut* 2020;**168**:310–22.
16. Yu J, Chen XQ, Chen LH, et al. Optimal scheduling of GEO debris removing based on hybrid optimal control theory. *Acta Astronaut* 2014;**93**:400–9.
17. Yu J, Chen XQ, Chen LH. Optimal planning of LEO active debris removal based on hybrid optimal control theory. *Adv Space Res* 2015;**55**(11):2628–40.
18. Bérend N, Olive X. Bi-objective optimization of a multiple-target active debris removal mission. *Acta Astronaut* 2016;**122**:324–35.
19. Huang PF, Zhang F, Ma J, et al. Dynamics and configuration control of the Maneuvering-Net Space Robot System. *Adv Space Res* 2015;**55**(4):1004–14.
20. Viavattene G, Devereux E, Snelling D, et al. Design of multiple space debris removal missions using machine learning. *Acta Astronaut* 2022;**193**:277–86.
21. Jorgensen MK, Sharf I. Optimal planning for a multiple space debris removal mission using high-accuracy low-thrust transfers. *Acta Astronaut* 2020;**172**:56–69.
22. Wang WL. Mission plan of active debris removal and design of guidance and control techniques applying space maneuver vehicle [dissertation]. Changsha: National University of Defense Technology, 2017 [Chinese].
23. Alfriend KT, Lee DJ, Creamer NG. Optimal servicing of geosynchronous satellites. *J Guid Control Dyn* 2006;**29**(1):203–6.
24. Madakat D, Morio J, Vanderpooten D. Biobjective planning of an active debris removal mission. *Acta Astronaut* 2013;**84**:182–8.
25. Yang JN, Hu YH, Liu Y, et al. A maximal-reward preliminary planning for multi-debris active removal mission in LEO with a greedy heuristic method. *Acta Astronaut* 2018;**149**:123–42.
26. Cerf M. Multiple space debris collecting mission—debris selection and trajectory optimization. *J Optim Theory Appl* 2013;**156**(3):761–96.
27. Novak DM, Vasile M. Improved shaping approach to the preliminary design of low-thrust trajectories. *J Guid Control Dyn* 2011;**34**(1):128–47.
28. Fan ZC, Huo MY, Qi J, et al. Fast initial design of low-thrust multiple gravity-assist three-dimensional trajectories based on the Bezier shape-based method. *Acta Astronaut* 2021;**178**:233–40.
29. Zuiani F, Vasile M. Preliminary design of debris removal missions by means of simplified models for low-thrust, many-revolution transfers. *Int J Aerosp Eng* 2012;**2012**:1–22.
30. Gao Y, Tian YL, Liu H, et al. Gaussian fitting based optimal design of aircraft mission success space using multi-objective genetic algorithm. *Chin J Aeronaut* 2020;**33**(12):3318–30.
31. Li YQ, Wang RX, Liu Y, et al. Satellite range scheduling with the priority constraint: An improved genetic algorithm using a station ID encoding method. *Chin J Aeronaut* 2015;**28**(3):789–803.
32. Liu Y, Yang JN. A multi-objective planning method for multi-debris active removal mission in LEO. Reston: AIAA; 2017. Report No: AIAA-2017-1733.
33. Zhou M, Sun S. *Genetic algorithms: Theory and applications*. 1st ed. Beijing: National Defense Industry Press; 1999. p. 6–10 [Chinese].